

Reconstruction of tunnel exit time and exit momentum in strong field ionization, based on phase space methods

Szabolcs Hack* and Attila Czirják†

*ELI-ALPS, ELI-HU Non-Profit Ltd., H-6720 Szeged, Dugonics tér 13, Hungary and
Department of Theoretical Physics, University of Szeged, H-6720 Szeged, Tisza L. krt. 84-86, Hungary*

Szilárd Majorosi and Mihály Benedict

Department of Theoretical Physics, University of Szeged, H-6720 Szeged, Tisza L. krt. 84-86, Hungary

(Dated: November 21, 2021)

INTRODUCTION

Strong field ionization of atoms plays a fundamental role in attosecond physics [1]: a suitably strong laser pulse enables an electron to leave (usually by tunneling) from its atomic bound state into the continuum, which is the first step of the very successful three-step model underlying our understanding of high-order harmonic generation and attosecond metrology. Currently, the problems of tunneling time [2] and exit momentum in tunnel ionization are of fundamental importance regarding both quantum theory and the interpretation of experimental results in attosecond physics. In the last few years, several groups published relevant experimental results [3–6], typically with the attoclock method. However, the interpretation of these measurements is usually difficult and there are also controversial results.

Isolated attosecond pulses can be generated by linearly polarized few- or single-cycle laser pulses if the electric field of the laser pulse exceeds a threshold value only during the half-cycle containing the peak [7]. Tunnel ionization is then possible practically only during this half-cycle. However, tunnel ionization produces an electron wavepacket which is blurred in space and time, thus attributing a classical particle to this wavepacket is rather ambiguous. Some of the electrons liberated by tunnel ionization ultimately leave the parent ion and can be detected later, while other electrons return to the parent ion and either rescatter on it or recombine with it. In this latter case, the emission of a high-energy photon with a proper phase is possible which contributes to the resulting macroscopic isolated attosecond pulse. Due to this probabilistic nature of this quantum process, the relative timing of the driving laser pulse and the generated attosecond pulse („time zero”) a priori can not be determined more accurately than a few tens of attoseconds, which leads to problems in the interpretation of experimental results in attosecond physics. In this contribution, we analyze tunnel ionization of a single atom based on the Wigner function over the classical phase space which inspires improved classical electron trajec-

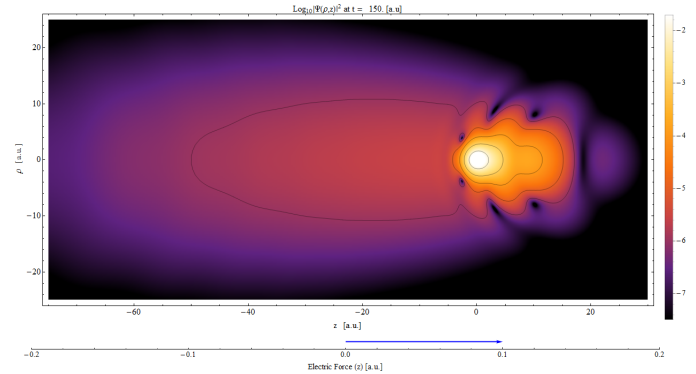


Figure 1. Density plot of the base 10 logarithm of the absolute square of the wave function of a tunneling electron at the instant of the peak of the laser pulse.

ries: these start with exit momenta based on the quantum momentum function and correspond very well to the subsequent quantum evolution.

THEORETICAL MODEL AND NUMERICAL SOLUTION

We work in the framework of a simple model: dipole approximation for the interaction of a single active electron atom with the classical electromagnetic field in the length gauge. We consider a near-infrared single-cycle laser pulse with sine-squared envelope, linearly polarized along the z -direction, which excites the electron from the ground state of the bounding atomic Coulomb potential. We solve the 3D time-dependent Schrödinger equation for the relative motion numerically, in cylindrical coordinates:

$$i\hbar \frac{\partial}{\partial t} \Psi = \left[-\frac{\hbar^2}{2m} \left(\frac{\partial^2}{\partial z^2} + \frac{\partial^2}{\partial \rho^2} + \frac{1}{\rho} \frac{\partial}{\partial \rho} \right) + V_{\text{core}}(z, \rho) + qE(t) \cdot z \right] \Psi \quad (1)$$

Our recently developed algorithm [8] supports the direct numerical integration of this TDSE with Coulomb-singularities and provides fourth order accuracy in both space and time coordinate steps. We show the probability density of the tunneling electron in Fig. 1.

* Szabolcs.Hack@eli-alps.hu

† czirjak@physx.u-szeged.hu

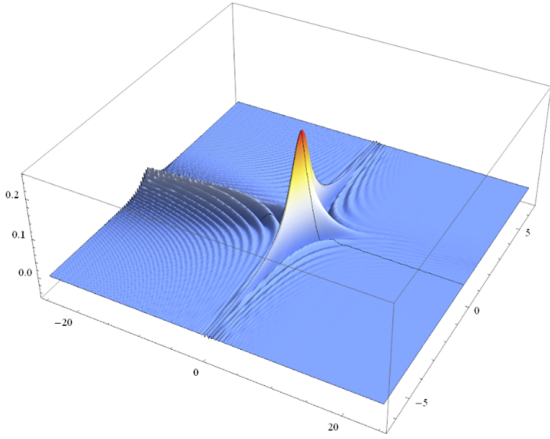


Figure 2. Color coded 3D plot of the Wigner function of the tunneling electron's quantum state along the direction of the laser polarization, shown at the instant of the peak of the laser pulse.

From the numerical solution, we first reduce the 3D wave function to the direction z (by integrating over ρ) and then we compute the corresponding Wigner function [9] as:

$$W(z, p_z, t) = \frac{1}{\pi} \int_{-\infty}^{\infty} d\zeta \exp(2ip_z\zeta) \Psi^*(z + \zeta, t) \Psi(z - \zeta, t). \quad (2)$$

We show the Wigner function in Fig. 2 at the instant of the peak of the laser pulse.

Based on the moments of the Wigner function

$$P_n(z, t) = \int p_z^n W(z, p_z, t) dp_z, \quad (3)$$

it is intuitive to obtain the quantum momentum function

$$\bar{p}_z(z, t) = \frac{P_1(z, t)}{P_0(z, t)} \quad (4)$$

which we next compare with classical trajectories.

RESULTS

In order to compare the classical and quantum dynamics of the tunnel ionization process, we compute the classical electron trajectories starting from the tunnel exit with non-zero exit momentum, given by the quantum momentum function, see Fig. 3. The motion is governed by the laser pulse according to the Newton-Lorentz equation:

$$\ddot{\mathbf{r}} = -q(\mathbf{E}(t) + \dot{\mathbf{r}}(t) \times \mathbf{B}(t)),$$

We compare the resulting classical motion along the direction of the laser polarization to the corresponding

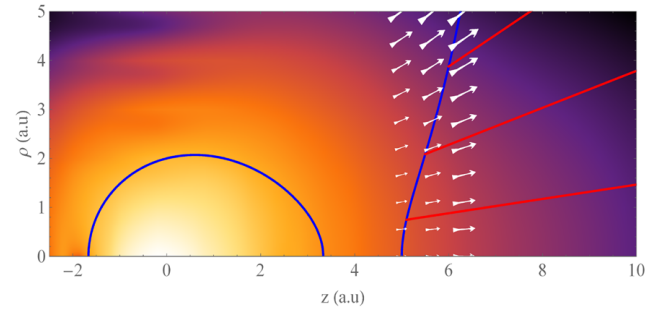


Figure 3. Plot of the real space electrons trajectories (red) starting with exit momenta (white arrows) based on the 3D quantum momentum function, on top of the density plot of the quantum probability density at the laser peak power. We plot the contours of the tunnel region in blue.

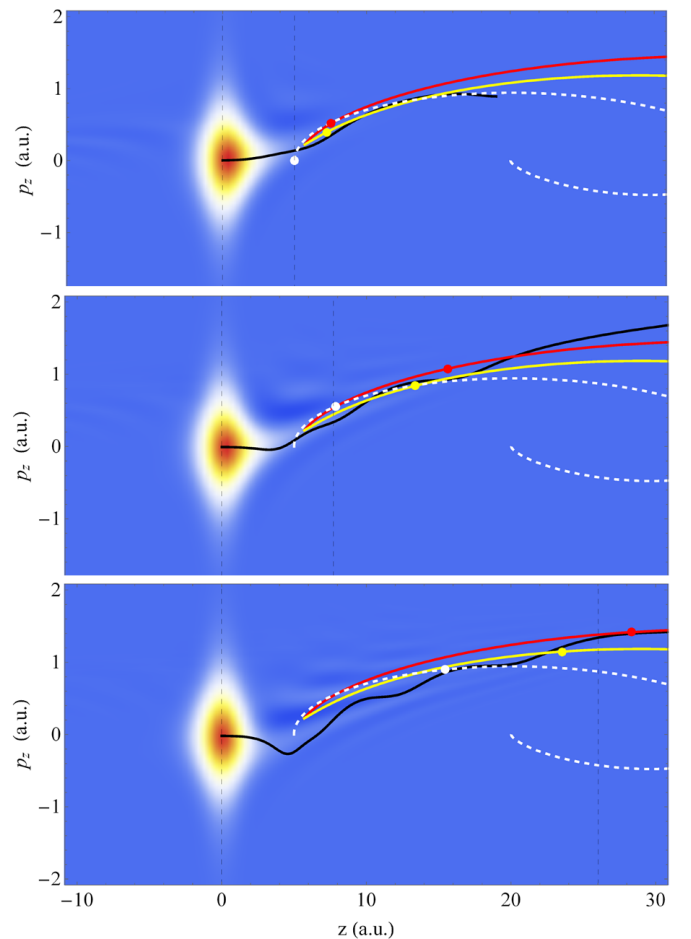


Figure 4. Time evolution of the phase space dynamics of an electron with tunnel exit time of 145 a.u., shown at time instants of 150, 160 and 170 a.u. We plot the classical trajectories of the simple-man model (white dashed), the improved trajectories with non-zero exit momentum with (yellow) and without (red) Coulomb-interaction, in comparison with the quantum momentum function (black) on top of the density plot of the Wigner function. Vertical dashed lines: positions of the ion core and tunnel exit.

quantum dynamics with the help of phase space trajectories and the Wigner function in Fig. 4.

Using the analytical solution of the Newton-Lorenz equation above, we obtain the following equations which we use to reconstruct approximately the tunnel exit time (t_i) and the exit momentum components (p_z^0 and p_ρ^0), based on the momentum components measured by a (e.g. TOF) detector (p_z^d and p_ρ^d):

$$p_z^0 = p_z^d \cos(\beta(t_i)) + (c - p_\rho^d) \sin(\beta(t_i)) \quad (5)$$

$$p_\rho^0 = c - (c - p_\rho^d) \cos(\beta(t_i)) + p_z^d \sin(\beta(t_i)), \quad (6)$$

$$\beta(t_i) = \frac{E_0}{16c\omega} \left[6 \sin\left(\frac{2}{3}\omega t_i\right) - 8 \sin(\omega t_i) + 3 \sin\left(\frac{4}{3}\omega t_i\right) \right]. \quad (7)$$

Based on our simulations, the relative errors for the reconstructed tunnel exit time and for the exit momentum component perpendicular to the laser polarization (p_ρ^0) are below 0.1%, and for the exit momentum component parallel to the laser polarization (p_z^0) below a few percent.

By detecting all those electrons which ultimately leave the atom, we can reconstruct the last tunnel exit time for such electrons, which is then also the start time for

those electrons which can recombine and thus contribute photons to the resulting isolated attosecond pulse.

CONCLUSIONS

We present some improvements to the description of optical tunneling and we show how to associate tunnel exit time and exit momentum to the classical trajectories based on the quantum momentum function. The resulting electron trajectories fit very well to the quantum description given by the Wigner function and by the quantum momentum function. Our results also show that the tunnel ionization starts a few atomic time units before the main peak of the linearly polarized single-cycle laser pulse. We also derived an approximate analytic formula to reconstruct the exit momentum and ionization time from electron momentum data measured with a usual time-of-flight electron detector. This also allows to determine an improved start time for those electrons that can recombine with the parent ion, which then may help to determine the "time zero" of the attosecond pulse.

-
- [1] F. Krausz and M. Ivanov, *Rev. Mod. Phys.* **81**, 163 (2009).
 - [2] A. S. Landsman and U. Keller, *Physics Reports* **547**, 1 (2015).
 - [3] P. Eckle, A. N. Pfeiffer, C. Cirelli, A. Staudte, R. Dörner, H. G. Muller, M. Büttiker, and U. Keller, *Science* **322**, 1525 (2008).
 - [4] D. Shafir, H. Soifer, B. D. Bruner, M. Dagan, Y. Mairesse, S. Patchkovskii, M. Y. Ivanov, O. Smirnova, and N. Dudovich, *Nature* **485**, 343 (2012).
 - [5] A. S. Landsman and U. Keller, *Journal of Physics B: Atomic, Molecular and Optical Physics* **47**, 204024 (2014).
 - [6] N. Camus, E. Yakaboylu, L. Fechner, M. Klaiber, M. Laux, Y. Mi, K. Z. Hatsagortsyan, T. Pfeifer, C. H. Keitel, and R. Moshhammer, *Phys. Rev. Lett.* **119**, 023201 (2017).
 - [7] M. Lewenstein, P. Balcou, M. Y. Ivanov, A. L'Huillier, and P. B. Corkum, *Physical Review A* **49**, 2117 (1994).
 - [8] S. Majorosi and A. Czirják, *Computer Physics Communications* **208**, 9 (2016).
 - [9] A. Czirják, R. Kopold, W. Becker, M. Kleber, and W. Schleich, *Optics communications* **179**, 29 (2000).